Virology 413 (2011) 72–83

Contents lists available at ScienceDirect

Virology

journal homepage: www.elsevier.com/locate/yviro

Accumulation of *Potato spindle tuber viroid*-specific small RNAs is accompanied by specific changes in gene expression in two tomato cultivars

Ying Wang [a], Makoto Shibuya [a], Akito Taneda [b], Tasuku Kurauchi [c], Mineo Senda [c], Robert A. Owens [d], Teruo Sano [a,e,*]

[a] *Plant Pathology Laboratory, Faculty of Agriculture and Life Science, Hirosaki University, Hirosaki 036-8561, Japan*
[b] *Graduate School of Science and Technology, Hirosaki University, Hirosaki 036-8561, Japan*
[c] *Faculty of Life Science and Agriculture, Hirosaki University, Hirosaki 036-8561, Japan*
[d] *Molecular Plant Pathology Laboratory, USDA/ARS, Beltsville, MD 20705, USA*
[e] *Gene Research Center, Hirosaki University, Hirosaki 036-8561, Japan*

ARTICLE INFO

Article history:
Received 14 October 2010
Returned to author for revision
7 November 2010
Accepted 14 January 2011
Available online 25 February 2011

Keywords:
RNA silencing
Small RNA
Large-scale sequencing
Transcript profiling
Microarray analysis
Viroids

ABSTRACT

To better understand the biogenesis of viroid-specific small RNAs and their possible role in disease induction, we have examined the accumulation of these small RNAs in potato spindle tuber viroid (PSTVd)-infected tomato plants. Large-scale sequence analysis of viroid-specific small RNAs revealed active production from the upper portion of the pathogenicity and central domains, two regions previously thought to be underrepresented. Profiles of small RNA populations derived from PSTVd antigenomic RNA were more variable, with differences between infected Rutgers (severe symptoms) and Moneymaker (mild symptoms) plants pointing to possible cultivar-specific differences in small RNA synthesis and/or stability. Using microarray analysis, we monitored the effects of PSTVd infection on the expression levels of >100 tomato genes containing potential binding sites for PSTVd small RNAs. Of 18 such genes down-regulated early in infection, two genes involved in gibberellin or jasmonic acid biosynthesis contain binding sites for PSTVd small RNAs in their respective ORFs.

Introduction

Viroids are the smallest known infectious agents and induce disease in a wide variety of plant hosts, including many crop species (Diener, 1987). Ranging in size from *ca.* 250–400 nucleotides (nt) replication of their single-stranded, circular, non-coding RNA genomes is entirely dependent on transcriptional and processing machinery supplied by the host (Daros and Flores, 2004); transport of the resulting progeny utilizes pre-existing cellular pathways. Their small size and unique molecular structure makes these molecules an attractive system with which to analyze many different aspects of host–pathogen interaction (Tabler and Tsagris, 2004; Flores et al., 2005a,b; Ding and Itaya, 2007).

The current ICTV classification scheme organizes the more than 30 recognized species of viroids into two families: members of the family *Pospiviroidae* contain a central conserved region and replicate in the nucleus; members of the family *Avsunviroidae* lack a central conserved region but exhibit hammerhead ribozyme activity and replicate in the chloroplast (Branch and Robertson, 1984; Flores et al., 2005a,b). Although replication occurs in different subcellular compartments, members of both families of viroids induce RNA silencing and the accumulation of viroid-specific small RNAs following infection (Itaya et al., 2001; Papaefthimiou et al., 2001; Martinez de Alba et al., 2002; Markarian et al., 2004).

Post-transcriptional gene silencing (RNA silencing) provides a multilayer defense system which protects plants from invasion by exogenous RNA replicons such as viruses and viroids (Vance and Vaucheret, 2001; Baulcombe, 2004; Herr, 2005; Molnar et al., 2005; Daros et al., 2006; Fusaro et al., 2006; Ruiz-Ferrer and Voinnet, 2009; Ding, 2010; Garcia-Ruiz et al., 2010; Molnar et al., 2010). Silencing is triggered by conversion of double-stranded or hairpin RNAs to small RNAs whose sizes ranging between 18 and 26 nucleotides (Elbashir et al., 2001; Hamilton et al., 2002). Infected plants contain high levels of viroid-specific small RNAs, but the circular genomic RNAs themselves appear relatively resistant to RNA silencing — raising the possibility that viroid replication may also be resistant (Itaya et al., 2007; Martín et al., 2007; Machida et al., 2007). The mechanism underlying this resistance/tolerance is not yet understood (Carbonell et al., 2008), but certain transgenic tomato lines expressing high levels of hairpin RNA-derived small viroid RNAs are resistant to infection (Schwind et al., 2009).

Viroid pathogenicity has long been analyzed in relation to the unique highly base-paired structure of the genomic RNA. *Potato*

* Corresponding author at: Plant Pathology Laboratory, Faculty of Agriculture and Life Science, Hirosaki University, Hirosaki 036-8561, Japan. Fax: +81 172 39 3817.
E-mail address: sano@cc.hirosaki-u.ac.jp (T. Sano).

0042-6822/$ – see front matter © 2011 Elsevier Inc. All rights reserved.
doi:10.1016/j.virol.2011.01.021

spindle tuber viroid (PSTVd) and related viroids contain five structural domains (Keese and Symons, 1985), and sequence changes located within the so-called "pathogenicity domain" have dramatic effects on PSTVd symptom expression (e.g., Schnölzer et al., 1985). It is important to note, however, that changes in the other four structural domains can also have significant effects on symptom development (Visvader and Symons, 1985; Sano et al., 1992; Rodriguez and Randles, 1993; Reanwarakorn and Semancik, 1998; Sano and Ishiguro, 1998; Qi and Ding, 2003), and an increasing body of evidence has begun to accumulate indicating that viroid-induced RNA silencing may play an important role in disease development. Several groups have described a positive correlation between symptom severity and the accumulation of small RNAs derived from PSTVd (Itaya et al., 2001; Matoušek et al., 2007) or *Avocado sunblotch viroid* (ASBVd) (Markarian et al., 2004). Symptom expression may also decease late in the infection when PSTVd-infected tomato plants have sometimes been observed to "recover" (Sano and Matsuura, 2004).

Several siRNAs derived from the leader sequence of *Cauliflower mosaic virus* (CaMV) 35S RNA exhibit near-perfect sequence complementarity to *Arabidopsis* transcripts, and, using a sensor transgene, Moissard and Voinnet (2006) were able to obtain direct evidence that at least one of those molecules acts as a bona fide siRNA in infected turnip. Additional bioinformatics searches identified >100 transcripts potentially targeted by CaMV-derived siRNAs, several of which are effectively down-regulated during infection. The first direct evidence for a role for RNA silencing in PSTVd symptom expression was provided by Wang et al. (2004) who reported that transgenic tomato lines expressing a non-infectious PSTVd hairpin RNA exhibit leaf symptoms very similar to those observed in infected plants. Recently, however, the significance of these observations was called into question by the failure of T3 progeny from certain of these transgenic lines to express similar symptoms (Schwind et al., 2009). Yet another indication of previously unsuspected complexity involves viroid infection in *Nicotiana benthamiana* where symptom expression in *Hop stunt viroid* (HSVd)-infected plants has been reported to be dependent upon the activity of RNA-directed RNA polymerase 6 (RDR6), an enzyme known to be involved in secondary small RNA synthesis (Gomez et al., 2008). Symptom expression in comparable PSTVd-infected plants, in contrast, is RDR6-independent (Di Serio et al., 2010).

In a previous study (Machida et al., 2007) we used northern hybridization analysis to monitor the accumulation of PSTVd-specific small RNAs (srPSTVds) in infected tomato plants. Shorter small RNA species (ca. 21 nt) were observed to accumulate early in the infection, whereas at later times both short and long (ca. 24 nt) small RNAs were present. Sequence information obtained from these srPSTVd populations using small-scale cloning/sequencing methods revealed the presence of several apparent "hot spots" located outside the pathogenicity domain, but these data were not completely consistent with the hybridization results. Comparatively few 24 nt srPSTVds were recovered from samples collected at either time, and others have reported similar results for tomatoes infected with either PSTVd (Itaya et al., 2007) or *Citrus exocortis viroid* (CEVd) ((Martín et al., 2007) as well as peach trees infected with *Peach latent mosaic viroid* (PLMVd) (St-Pierre et al., 2009). For small RNAs derived from both the viroid plus (genomic) and minus (antigenomic) strands a large majority of the molecules recovered from infected plants contained 21–22 nt. In addition to infected tomato, srPSTVd synthesis has also been examined in two other experimental systems; i.e., transgenic tomatoes expressing a non-infectious PSTVd hairpin RNA transcript (Schwind et al., 2009) as well as PSTVd-infected *N. benthamiana* containing either normal or reduced levels of RDR6 (DiSerio et al., 2010). Certain quantitative differences notwithstanding, the srPSTVd populations recovered from these various sources appear quite similar.

In this study we have examined the accumulation pattern and size distribution of PSTVd-specific small RNAs of both polarities in the leaves and stems of infected tomato plants using northern hybridization and also carried out large scale sequencing analyses of viroid-specific small RNAs isolated from leaf tissue. Here, we present data providing a more comprehensive profile of viroid-specific small RNA accumulation in infected tissue, profiles in which PSTVd-specific small RNAs are abundantly produced from both the pathogenicity domain and the central conserved region of the viroid. Microarray analysis of the changes in host gene expression accompanying PSTVd infection has identified several potential targets for RNA silencing mediated by these small RNAs.

Results

Accumulation patterns of PSTVd-specific small RNAs in leaves and stems

Three weeks post inoculation (wpi), when epinasty (leaf curling) had begun to appear in the third or fourth true leaves, individual leaves and the corresponding stem segments from six PSTVd-infected tomato seedlings were harvested and then pooled for extraction of LMW RNA (Fig. 1A). Aliquots of the resulting LMW RNA preparations (2 μg) were then fractionated by electrophoresis in a 12% polyacrylamide gel containing 8 M urea (Fig. 1B-(1)), and the accumulation of srPSTVds having either genomic (+) (Fig. 1B-(3) left) or anti-genomic (−) (Fig. 1B-(3) right) polarity was analyzed by northern hybridization. As previously reported (Machida et al., 2007), two major classes of (+)srPSTVd (estimated sizes = ca. 21–22 and 24 nt) were easily detected; in contrast, only a single species of (−)srPSTVd (ca. 21–22 nt) was visible (Fig. 1B-(3) arrows).

Even though the same amount of LMW RNA (calculated on the basis of A260 UV absorbance value) was applied to each lane in Fig. 1B-(1), note that the intensity of the resulting srPSTVd signals was consistently higher for samples isolated from stem tissue. When signal intensities for srPSTVds between 20 and 24 nt in size were quantified and normalized against the amount of tRNA present (Fig. 1B-(1), upper arrow), data presented in Fig. 1C indicated that (+)srPSTVd concentrations were 4.8–26.2-fold higher in stems as compared to leaf tissue. For (−)srPSTVd the corresponding ratios were slightly lower; i.e., 1.8–6.6-fold. Normalization against the relative amounts of PSTVd progeny as determined by Northern analysis (see Fig. 1B-(2)) yielded similar results (not shown).

Large-scale sequence analysis of srPSTVd populations

Two different sets of large-scale srPSTVd sequence analyses were carried out. Our first large-scale sequence analyses comparing small RNA populations recovered from stem and leaf tissue harvested 3 wpi yielded a total of 2,082,822 (stem) and 6,132,729 (leaf) reads having the expected lengths of 15–29 nt. While 86.4% of the sequences recovered from stem tissue were >20 nt long, more than half of those recovered from leaf tissue (i.e., 3,423,284) were <19 nt in length. This difference probably reflects the presence of relatively high levels of RNAs smaller than tRNA in RNA isolated from leaf tissue (see Fig. 1B-(1), lower arrow). For the stem sample, comparison of sequence reads 15–29 nt in length to the sequences of PSTVd genomic (+) and anti-genomic (−) strands yielded a total of 89,070 and 1779 srPSTVds, respectively. Comparable totals for the leaf sample were 2205 and 491.

The mature circular genomic RNA of PSTVd (and other viroids) is often assumed to provide the major substrate for small RNA synthesis. Results from studies by Gas et al. (2007, 2008) indicate, however, that DCL also recognizes the multimeric (+)strand RNAs synthesized during replication of CEVd and related viroids, cleaving these molecules between positions 95–96 in the upper central conserved region to release monomeric linear progeny. To gain insight into the substrates and pathway(s) involved in srPSTVd production, we first mapped the distribution of srPSTVds recovered from stem and leaf samples onto the sequences of the respective substrate strand.

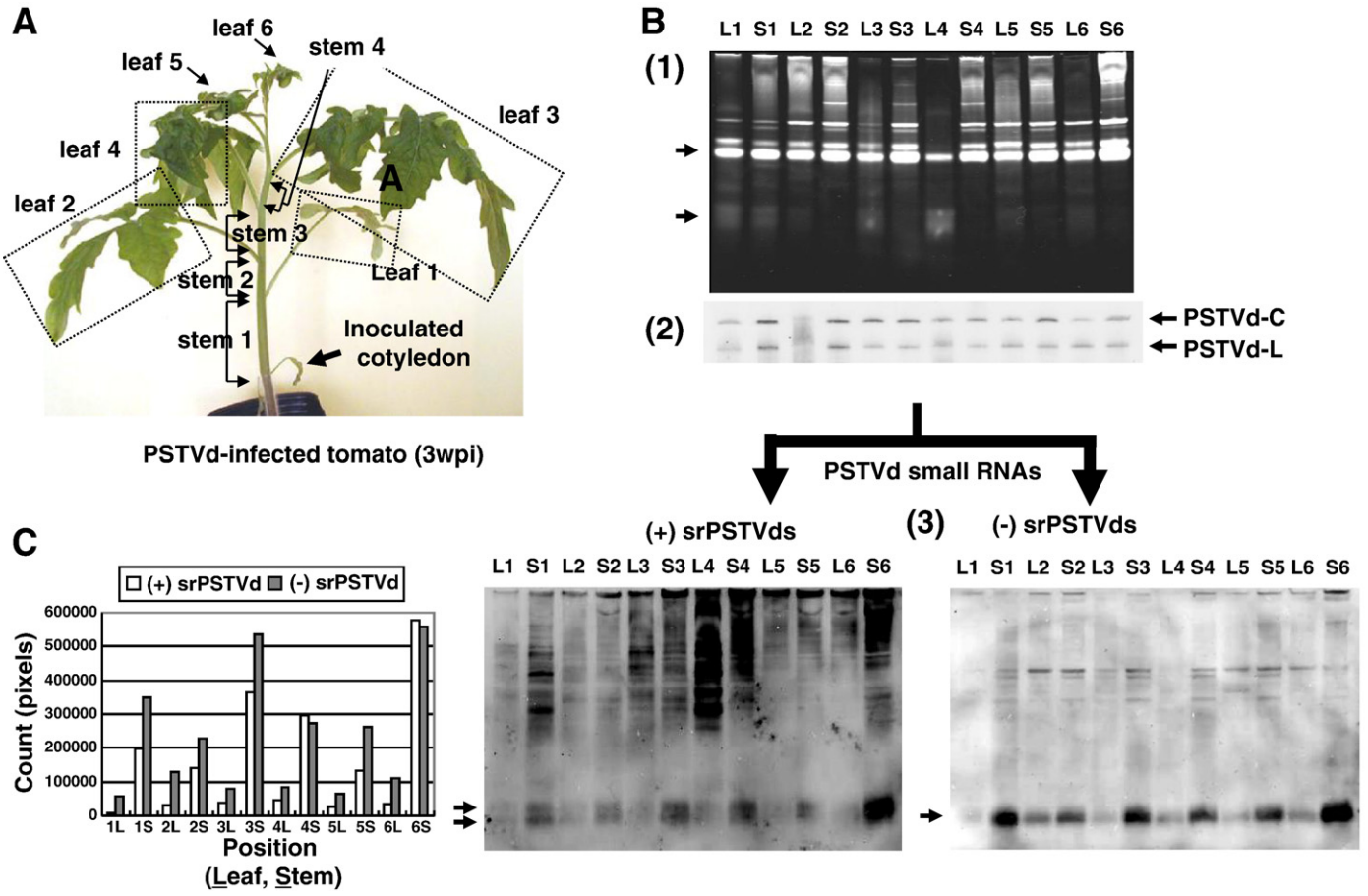

Fig. 1. Relative concentrations of (+) and (−)srPSTVd in infected Rutgers tomato. (A) Photograph of diseased plant taken three weeks post-inoculation. Note the presence of epinasty in the lower leaflets of leaf 3. (B) Aliquots (2 μg) of LMW RNA isolated from leaves 1–6 and the corresponding internodes were fractionated by denaturing PAGE and then either stained with ethidium bromide (1) or transferred to nylon membrane and hybridized with DIG-labeled PSTVd-cRNA probes specific for the genomic PSTVd RNAs (2) or for srPSTVds derived from the genomic ((3)-left panel) or anti-genomic ((3)-right panel) RNA. Two size classes of (+)srPSTVd (left panel, two arrows) were consistently present. (C) Comparison of srPSTVd levels after normalization against the amount of tRNA as determined by ethidium bromide staining (see the upper arrow in panel B-(1)). Levels of (+) and (−)srPSTVds in stems were 4.8–26.2 and 1.8–6.6x higher than in the leaves, respectively.

Comparison of the individual profiles shown in Fig. 2 indicated that the (+) and (−)srPSTVds originate from largely non-overlapping portions of the genome. Major peaks of (+)srPSTVds were visible at positions 30–60 and 90–110 in the so-called "upper strand" with 1–2 smaller peaks possibly centered around positions 270 and 320 in the opposing "lower strand". Most (−)srPSTVds, in contrast, were derived from the lower strand and right terminal loop (positions 160–320).

Despite certain quantitative differences, corresponding profiles for srPSTVds isolated from stems and leaves appeared qualitatively similar. Of particular interest was the relatively large amount of (+)srPSTVd derived from the pathogenicity domain; i.e., positions 30–60 in the upper strand and, to a lesser extent, positions 290–310 in the lower strand (see Fig. 2B (a)). Previous small-scale analyses (e.g., Machida et al., 2007) had failed to detect this apparent hotspot. Vertical arrows in Fig. 2B (a, b) denote the 5′ termini of two other small RNAs whose presence suggests that alternative structural interaction may play an important role in dicer targeting to PSTVd. Formation of the so-called "trihelical processing structure" involving position 95–96 by PSTVd genomic RNA (Diener, 1986; Baumstark et al., 1997; Gas et al., 2007) as well as secondary hairpin II by the antigenomic RNA (Loss et al., 1991) is considered in greater detail below (see Discussion).

Cultivar-specific differences in srPSTVd populations isolated from leaf tissue

Previous studies of disease induction by PSTVd (and other viroids) have focused almost exclusively on visible symptoms like stunting, epinasty, and necrosis that appear in the foliage of Rutgers or other sensitive tomato cultivars. The number of srPSTVd sequences recovered from Rutgers leaf tissue in our first large-scale sequence analysis was too small to allow any firm conclusions about the possible role of srPSTVd-mediated gene silencing in symptom development. A much larger number of sequences were recovered from stem tissue, but even here the data were still quite limited and not adequate to characterize the pathway(s) of srPSTVd formation.

To address these problems, five additional large-scale sequence analyses were carried out using preparations of gel-purified small (15–30 nt) RNAs isolated from different leaf sources. In addition to healthy and PSTVd-infected Rutgers plants, leaf tissue was also collected from a second tomato cultivar (i.e., Moneymaker) in which symptom expression is much less pronounced. For the Moneymaker samples, leaf tissue was collected from healthy plants, PSTVd-infected plants, and transformed line IR11-14 which constitutively expresses srPSTVd RNA in the absence of viroid replication (Wang et al., 2004). Northern blot analyses of the genomic PSTVd RNAs and srPSTVds in these five RNA preparations indicated that the genomic circular and linear PSTVd RNAs were present only in PSTVd-infected Rutgers and Moneymaker tissues, but considerable amount of srPSTVds were also visible in the transformed Moneymaker in addition to those in PSTVd-infected Rutgers and Moneymaker tissues (Supplementary Figure S1). In addition to large scale sequence analysis of their small RNA populations, total RNA isolated from the young, still-expanding leaf tissue was also subjected to microarray analysis to monitor changes in

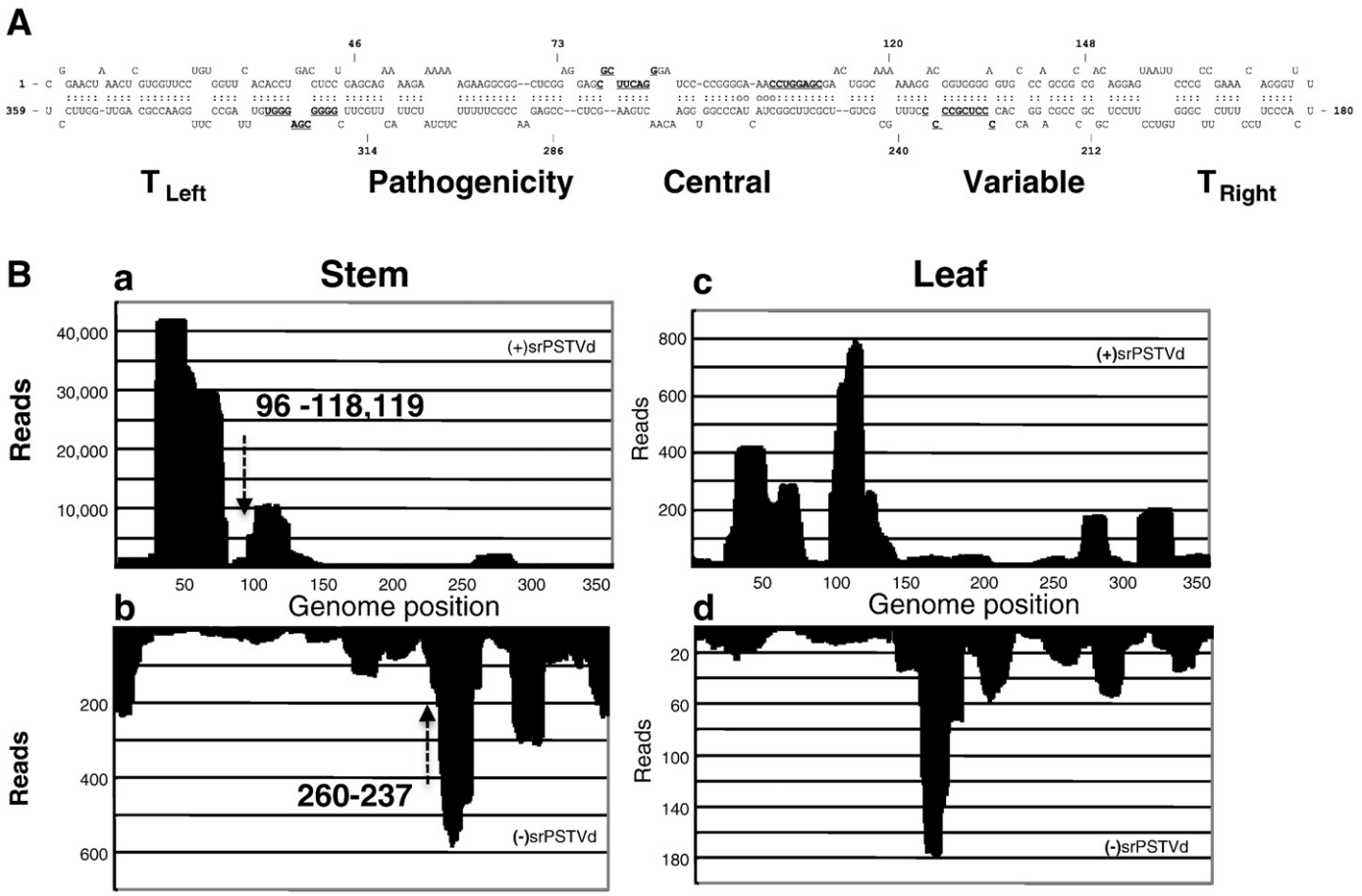

Fig. 2. Sequence profiles of (+) and (−)srPSTVd populations recovered from stem (a,b) and leaf (c,d) tissue of infected Rutgers plants. Bold vertical arrows denote the 5′ termini of two srPSTVds of particular interest; i.e., a (+)srPSTVd at position 96 and a (−)srPSTVd at position 237. Note the use of different scales to compensate for the lower numbers of (−) srPSTVd sequences recovered.

host gene expression associated with either PSTVd infection (infected Rutgers and Moneymaker) or srPSTVd synthesis in the absence of replication (transformed Moneymaker line IR14).

Unlike the earlier study comparing infected Rutgers stem and leaf tissue, these five analyses yielded large numbers of PSTVd-specific sequences. As shown in Table 1, each analysis yielded >20 million reads with virtually no PSTVd-related sequences detected in either of the samples from healthy leaf tissue. The three other samples each contained 2–3 million PSTVd-specific reads, a number representing approximately 10% of all small RNAs between 15 and 45 nt in length. Small RNAs derived from the genomic strand were consistently more abundant than those derived from PSTVd antigenomic RNA, and this ratio increased dramatically (>5 fold) in PSTVd-infected Rutgers plants. A large majority of (+) and (−)srPSTVd RNAs were 21–22 nt in length, and Fig. 3 shows the distribution patterns of these shorter molecules in all five samples. For a complete summary of data for all srPSTVds between 15 and 45 nt in length please see Supplementary Figures S2–S6.

Comparison of the panels in the two rightmost columns of Fig. 3 reveals striking similarities in the profiles of both (+) and (−) srPSTVds recovered from the leaves of PSTVd-infected and transgene-containing (but uninfected) Moneymaker plants. Comparison of the upper two panels in each column (21 and 22 nt in length) reveals that, on average, the most abundant size class of srPSTVds in the transgene-containing leaf tissue was 21 nt, which was 1 nt shorter than those in PSTVd-infected tissue; i.e., 21 vs. 22 nt. The most abundant size class of viroid small RNAs was also 22 nt in PSTVd-infected *N. benthamiana* (DiSerio et al., 2010), but 21 nt in HSVd- and GYSVd-infected grapevine (Navarro et al., 2009), HSVd-infected cucumber (Martinez et al., 2010), and PLMVd-infected peach trees (DiSerio et al., 2009). Multiple Dicer-like enzymes involved in cleavage may act differently on replicating viroid RNA and non-replicating transcribed viroid sequences. The overall profiles for both (+) and (−) srPSTVds appeared virtually identical, however. Turning our attention to the populations in PSTVd-infected Rutgers leaf tissue a much different situation is observed. Although the profile of (+)srPSTVds in this sample was quite similar to those seen for the Moneymaker samples, the population of (−)srPSTVds appeared to be much less diverse. As described in Table 1, levels of (−)srPSTVd in infected Rutgers leaf tissue were approximately 5-fold lower than those observed in comparable Moneymaker samples. Furthermore, two major clusters of (−) srPSTVds present in Moneymaker plants (i.e., those located near positions 200 and 300 and labeled “B” and “D” in Fig. 3) were

Table 1
PSTVd-related short sequence reads recovered from leaf tissue.

Sample	Total reads	PSTVd specific	Ratio (+/−)
Rutgers_Healthy	21,836,639	688 (+) 1414 (−)	–
Rutgers_PSTVd	21,131,951	2,041,081 (+) 237,682 (−)	8.59
Moneymaker_Healthy	21,929,222	194 (+) 127 (−)	–
Moneymaker_PSTVd	23,873,636	1,171,499 (+) 881,366 (−)	1.33
Moneymaker_IR14	24,103,693	1,824,430 (+) 1,107,942 (−)	1.64

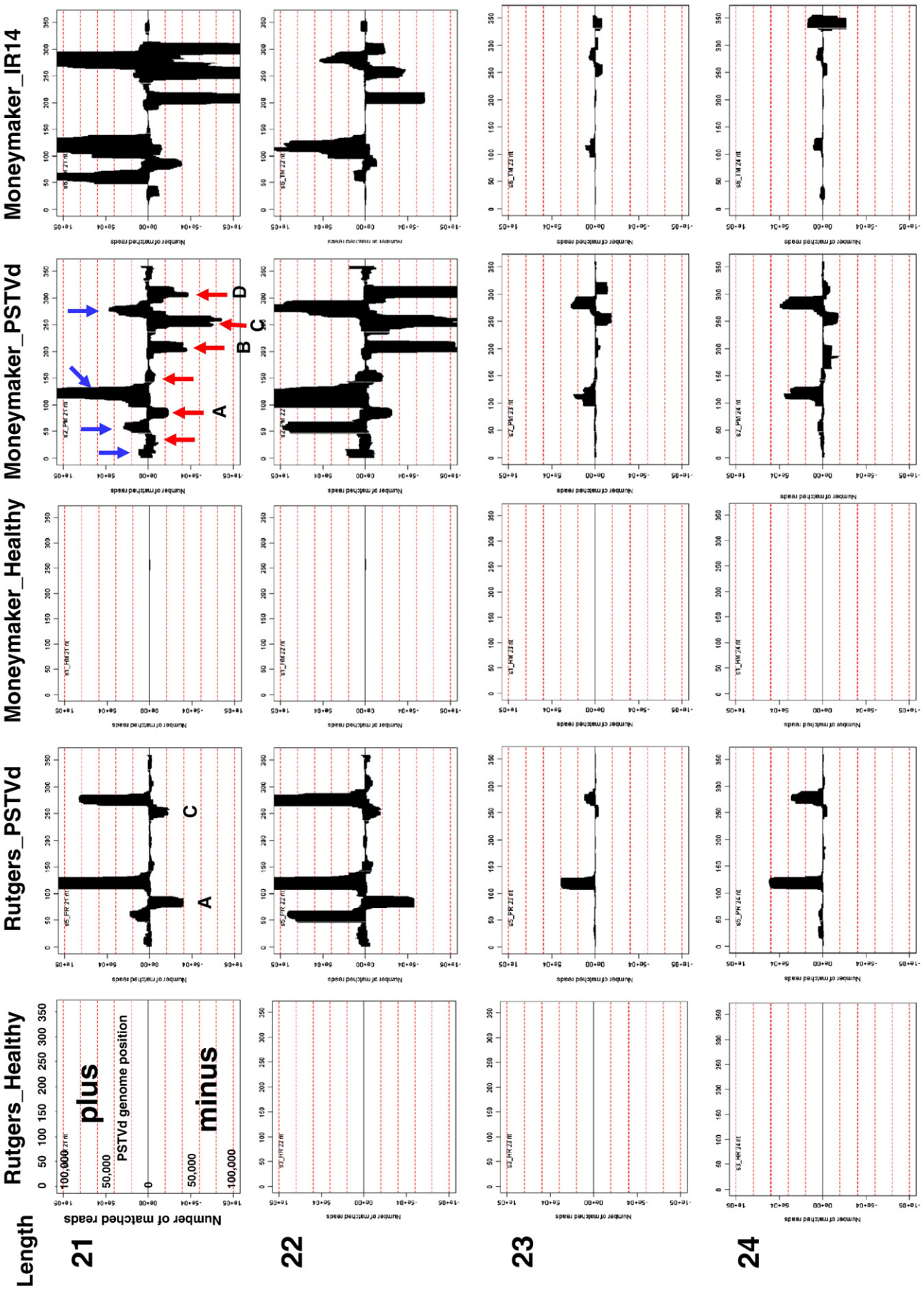
Rutgers_Healthy
Rutgers_PSTVd
Moneymaker_Healthy
Moneymaker_PSTVd
Moneymaker_IR14
Length
21
22
23
24
Number of matched reads
plus
minus
100,000
50,000
0
50,000
100,000
PSTVd genome position
A
B
C
D

virtually absent from Rutgers. Interestingly, only a relatively minor degree of overlap was observed in the location of each of the peaks of (+) and (−)srPSTVds recovered from these three samples.

Identification of potential targets of srPSTVd-mediated gene silencing

If srPSTVds do indeed regulate symptom expression via RNA silencing, one would expect to find i) complementary target sequence (s) in one or more host mRNAs and ii) decreased levels of these mRNAs in infected tissue. To search for evidence supporting such a scenario, we divided the PSTVd genomic and anti-genomic RNAs into series of 359 overlapping 21-nt RNAs and then compared sequences of these hypothetical srPSTVds with the latest tomato genome release using the miRNA target prediction tool available on the Tomato Functional Genomics Database. This process identified a total of 470 tomato unigenes as possible targets of small RNA regulation; i.e., 241 unigenes as targets for (+)srPSTVd and 234 unigenes as targets for (−) srPSTVd. Five unigenes were potentially targeted by both types of srPSTVd. As shown in Fig. 4, many of these potential interactions involved srPSTVds originating from the pathogenicity domain.

Next, microarray analysis was used to monitor changes in gene expression associated with PSTVd infection. The Rutgers and Moneymaker seedlings used for this experiment were older than those used for the first set of srPSTVd analysis described above, and plants were inoculated on the third true leaf rather than on the cotyledons. Typical symptoms of PSTVd infection (i.e., epinasty and stunting) began to appear in leaves 6–7 approximately two weeks post inoculation, and 13 days later systemically infected tissue was collected from the not-yet-fully-expanded leaf 11 for isolation of total RNA. This analysis was part of a larger study to be described in detail elsewhere (Owens RA, Tech KB, Shao JY, Sano T, and Baker CJ, unpublished data), and only selected results are presented below.

Each treatment contained four biological replicates, and the use of Affymetrix oligonucleotide arrays allowed us to monitor transcript levels for >10,000 tomato genes. Analysis of the resulting data sets revealed that expression of nearly one quarter of all genes in the Rutgers plants were significantly affected by PSTVd infection. Transcript levels for 242 genes were ≥2-fold up-regulated, and 292 genes were ≥2-fold down-regulated; 1977 other genes were less-dramatically (but still significantly) affected. Of 129 tomato unigenes represented on the array that contained potential srPSTVd target sites, less than one-third (i.e., 42/129) showed a significant response to PSTVd infection. As shown in Table 2, the genes affected represent a wide range of metabolic and regulatory pathways, and we note that their predicted srPSTVd target sites are concentrated in the respective coding regions (26/42) and/or 3′-UTRs (13/42). Almost evenly divided between srPSTVds derived from genomic and anti-genomic RNA, nearly two-thirds of the potential target sites are complementary to small RNAs derived from the PSTVd pathogenicity domain.

If disease induction were a direct result of srPSTVd-mediated down-regulation of host gene expression, one might expect i) lower levels of the targeted mRNA(s) in infected tissue and ii) at least a rough correlation between mRNA levels, disease severity, and the relative concentrations of specific srPSTVds in different cultivars. To look for evidence supporting such a scenario, we focused our attention on eight genes that showed significant changes in both Rutgers and Moneymaker plants. Of 18 genes initially identified as potential targets of srPSTVd-mediated down-regulation in infected Rutgers (Table 2), only five were also significantly down-regulated in Moneymaker plants. Two of these genes (i.e., gibberellin beta-hydroxylase and a copper chaperone-related, metal ion-binding protein) were also down-regulated in transgenic Moneymaker line IR14 that expresses severe symptoms in the absence of PSTVd replication.

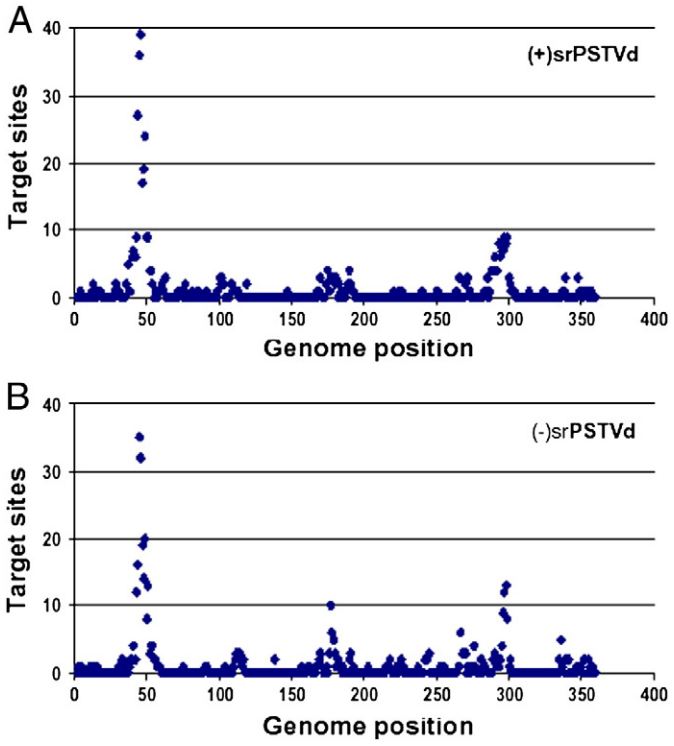

Fig. 4. Locations of srPSTVds potentially targeting tomato mRNAs. Hypothetical 21-nt srPSTVds derived from either the genomic (A) or anti-genomic (B) RNA were compared to the draft sequence of the tomato genome using the miRNA target prediction algorithm developed by Jones-Rhoades and Bartel (2004). For each hypothetical srPSTVd, the resulting number of potential target sites is plotted against the location of its 5′-terminus.

Gibberellin beta-hydroxylase and omega-3-fatty acid desaturase (a third down-regulated gene) play key roles in the biosynthesis of two different plant hormones, one of which (i.e., gibberellin) has been implicated in viroid symptom development. Lower levels of gibberellin beta-hydroxylase (and, therefore, active gibberellins) could explain the stunting seen in infected Rutgers and transgenic Moneymaker plants, but the fact that infected Moneymaker plants remained almost unaffected indicates that any effects of PTGS induced by PSTVd-derived small RNAs are likely to be complex/indirect. Infected Rutgers and Moneymaker plants contain similar levels of (+) srPSTVds potentially targeting gibberellin hydroxylase, and levels of (−)srPSTVds targeting the fatty acid desaturase involved in jasmonic acid biosynthesis were actually lower in the cultivar Rutgers where disease was most pronounced. And finally, we note that not all genes containing potential binding sites for srPSTVd were down-regulated; indeed, one gene encoding ethylene-induced EIX receptor 1 was strongly up-regulated in all three types of plants examined. In contrast to down-regulated genes where most predicted target sites were located in the ORF, target sites in all three up-regulated genes were located in the 3′-UTR.

Discussion

Viroid-infected plants accumulate significant levels of viroid-specific small RNAs containing 20–24 nucleotides, and recently

Fig. 3. Sequence profiles of srPSTVd populations recovered from leaves of infected and PSTVd transgene-containing tomatoes used for microarray analysis. From left to right, healthy Rutgers; PSTVd-infected Rutgers; healthy Moneymaker; PSTVd-infected Moneymaker; and, finally, transgenic Moneymaker line IR11-14 (Wang et al., 2004). From top to bottom, profiles for srPSTVds containing 21–24 nt are shown. Specific peaks of (−)srPSTVd discussed in the text are numbered. Because the transgene present in the IR11-14 plants contains a less-than-full-length PSTVd cDNA construct, these plants do not contain any full-length infectious progeny RNA.

Table 2
Possible srPSTVd-mediated effects on gene expression in different tomato cultivars.

SGN no.	Affymetrix probe set	Expression change[a] [Log2]	SOL annotation	srPSTVd polarity [b]	Target site
Down-regulated					
SGN-U563049	LesAffx.54718.1.S1_at	−1.666	AG-motif binding protein-1 [*N. tabacum*]	−(44)	ORF
SGN-U577578	Les.2012.1.S1_at	−1.262	Inositol-3-phosphate synthase, putative	+(300)	3′UTR
SGN-U563666	Les.2423.1.A1_at LesAffx.7704.1.S1_at	−1.244 −1.261 [−0.861/−1.282]	Metal ion-binding, copper chaperone (CCH)-related	+(44,45,48)	ORF
SGN-U578586	Les.3995.1.S1_at	−0.951 [−0.641/NS]	Glutamate permease	+(43,45)	3′UTR
SGN-U575510	Les.3967.1.S1_at	−0.873 [−0.516/NS]	Omega 3 fatty acid desaturase	−(266,265,264)	ORF
SGN-U578331	LesAffx.18025.1.S1_at	−0.728 [−0.740/−1.248]	Giberellin beta-hydroxylase	+(118)	ORF
SGN-U580429	Les.4583.1.S1_at	−0.709	NAD-dependent epimerase	−(48,47)	3′UTR
SGN-U571962	Les.4791.1.S1_at	−0.669	None	+(174)	ORF
SGN-U584595	Les.1784.2.A1_at	−0.655	Sugar transporter, putative	+(188,189,190,191)	ORF
SGN-U580321	Les.5120.1.S1_at	−0.587	NADPH : protochlorophyllide oxido-reductase [*N. tabacum*]	+(298)	ORF
SGN-U567353	Les.5143.1.S1_at	−0.512	Phosphatase, protein phosphatase 2A	−(254)	ORF
SGN-U580830	LesAffx.16204.1.S1_at LesAffx.16204.2.S1_at	−0.480 −0.416 [−0.673/NS]	FKBP-type peptidyl-prolyl cis–trans isomerase family protein	+(351,352,353)	ORF
SGN-U570097	LesAffx.55473.1.S1_at	−0.417	None	+(40,41,42,43,44,45)	ORF
SGN-U578545	LesAffx.70554.1.S1_at	−0.409	Kelch repeat-containing protein	+(265) −(339,338,340)	3′UTR
SGN-U574490	Les.4545.1.S1_at	−0.382	DnaJ protein, ARG1	+(292)	ORF
SGN-U585034	Les.5645.1.S1_at	−0.370	None	+(45,46,47)	3′UTR
SGN-U585132	LesAffx.10653.1.S1_at	−0.294	ARF GAP-like zinc finger-containing protein ZIGA3 (ZIGA3)	−(192,190)	ORF
SGN-U585135	Les.409.2.S1_at Les.409.3.S1_at	−0.280 −0.347	Steroid nuclear receptor, ligand-binding [*Medicago truncatula*]	−(111,110)	ORF
Up-regulated					
SGN-U576646	Les.2686.1.A1_at	0.244	*Clostridium pasteurianum* ferredoxin homolog [Solanum tuberosum]	−(42)	ORF
SGN-U578875	Les.5016.1.S1_at	0.297	Adenylosuccinate synthetase (ADSS),	−(47,46)	ORF
SGN-U586259	Les.5639.1.S1_at	0.299	Metaxin-related, contains 1 transmembrane domain	+(298)	ORF
SGN-U579979	Les.5125.1.S1_at	0.343	PUR alpha-1 protein	+(37,38,39)	3′UTR
SGN-U579812	LesAffx.630.1.A1_at	0.348	ARP protein (REF), identical to ARP protein GB (NADPH oxidoreductase)	+(294)	5′UTR
SGN-U568908	Les.5248.1.S1_at	0.368	None	+(107,108,111,112)	5′UTR
SGN-U585120	Les.2718.1.S1_at	0.370	6-Phosphogluconate dehydrogenase [*Arabidopsis thaliana*]	−(282)	5′UTR
SGN-U565153	Les.2328.1.A1_at	0.418	None	−(177,176,175)	5′UTR
SGN-U583104	Les.418.1.S1_at	0.433	Heat shock 70 kDa protein (mitochondria)	−(113)	ORF
SGN-U562778	LesAffx.67281.1.S1_at	0.441 [0.661/NS]	F-box family protein	+(99)	3′UTR
SGN-U578712	Les.3421.2.S1_at	0.447	60S ribosomal protein L5	+(182)	ORF
SGN-U574150	Les.476.2.S1_at Les.476.1.S1_at	0.457 0.382	Pescadillo-related, similar to pescadillo (Zebrafish, *Danio rerio*)	−(46,45)	ORF
SGN-U580537	Les.246.1.S1_at	0.459 [0.666/NS]	Fructose-bisphosphate aldolase	+(50)	3′UTR
SGN-U563879	LesAffx.51224.2.S1_at	0.468	None	−(45,44)	3′UTR
SGN-U581958	Les.390.2.S1_at Les.390.1.S1_at	0.485 0.372	Petunia Shaggy kinase 4 [*Petunia x hybrida*]/similar to glycogen synthase kinase-3	−(45,44)	ORF
SGN-U572830	Les.5514.1.S1_at	0.561	E3 ligase-like protein induced by chitin oligomers	−(53,52,51)	ORF
SGN-U564920	Les.1131.1.S1_at	0.563	Nucleosome assembly protein (NAP)	−(44)	ORF
SGN-U583406	Les.581.1.A1_at	0.571	Nucleolar essential protein-related	−(48,46,45,44,43)	ORF
SGN-U563134	Les.2267.1.S1_at	0.582	WD-40 repeat protein	+(294,295,296)	3′UTR
SGN-U577901	Les.319.1.A1_at	0.638	MAR-binding protein [*N. tabacum*]	−(44)	ORF

Table 2 *(continued)*

SGN no.	Affymetrix probe set	Expression change[a] [Log2]	SOL annotation	srPSTVd polarity [b]	Target site
SGN-U577993	Les.3706.1.S1_at	0.779	Indoleacetic acid-induced protein 3 (IAA3)	+(45,46,47)	3′UTR
SGN-U578450	Les.292.1.S1_at	1.438	N-rich protein [*Glycine max*]/ putative role in programmed cell death, hypersensitive response	−(44,43,40)	ORF/3′ UTR
SGN-U573229	Les.2137.1.S1_at	4.0133 [2.612/3.203]	EIX receptor 1 [*Lycopersicon esculentum*]	+(59)	3′UTR
SGN-U581430	Les.3635.1.S1_at	5.296	Cucumisin-like serine protease (ARA12, Asp48	−(335)	ORF

[a] Above, values for PSTVd-infected Rutgers plants; below (in brackets), values for PSTVd-infected (left) and IR11-14 transgenic (right) Moneymaker plants; NS, not significant.
[b] + and −, small RNAs derived from PSTVd genomic or anti-genomic RNA, respectively; locations of their respective 5′ termini are shown in parentheses.

published large-scale sequencing studies have examined the small RNA populations isolated from several different viroid–host combinations. As observed in earlier small-scale studies with PSTVd-infected tomato (e.g., Itaya et al., 2007; Machida et al., 2007), the profiles of small viroid-related RNAs isolated from HSVd- and GYSVd-infected grapevine (Navarro et al., 2009), HSVd-infected cucumber (Martinez et al., 2010), PLMVd-infected peach (Bolduc et al., 2010), and PSTVd-infected *N. benthamiana* (DiSerio et al., 2010) all contain one or more hotspots. Detailed analysis of this data suggests that cleavage probably involves different Dicer-like enzymes, and comparison of small RNA populations recovered from HSVd-infected cucumber leaf tissue and phloem exudate raises the possibility of selective trafficking of small viroid-related RNAs to/from the phloem (Martinez et al., 2010).

In the present study, we have compared the profiles of srPSTVd populations recovered from leaf tissue of PSTVd-infected Rutgers and Moneymaker plants as well as transformed (but uninfected) Moneymaker plants constitutively expressing srPSTVd. The greatest degree of similarity was observed among the respective (+)srPSTVd populations where each profile was seen to contain prominent hotspots derived from positions 40–60 and 90–130 in the upper portions of the pathogenicity or central-variable domains. A smaller data set derived from stem tissue collected from infected Rutgers plants yielded a qualitatively similar profile, and all four profiles were quite different from that observed by DiSerio et al. (2010) for (+) srPSTVds isolated from infected *N. benthamiana* leaf tissue. Turning to small RNAs derived from the PSTVd antigenomic strand, several striking differences were readily apparent. For example, Moneymaker plants (transgenic as well as PSTVd-infected) appeared to contain several-fold more (−)srPSTVd than comparable Rutgers plants; furthermore, while the (−)srPSTVd profiles from infected and transgenic Moneymaker plants were quite similar, certain (−) srPSTVds were much less abundant in the cultivar Rutgers. Rather than the three hotspots visible between positions 200–300 in the two Moneymaker profiles, the corresponding Rutgers profile in Fig. 3 contain just a single peak. These differences are in sharp contrast to the relatively similar levels of yet another group of (−)srPSTVds derived from positions 70–100.

As discussed in detail by Ding (2010), the pattern of (+) and (−) strand small RNA synthesis observed for many viruses strongly supports a model in which dsRNA replicative intermediates rather than highly-structured portions of the single-stranded genomic RNA provide the major substrate for siRNA synthesis. Such a model readily accounts for the presence of approximately equimolar amounts of (+) and (−)srPSTVds in PSTVd-infected as well as transgenic Moneymaker plants. As the substrate(s) for DCL are likely to be identical in both cultivars, the lower levels of (−)srPSTVds in infected Rutgers plants and different pattern of (−)srPSTVd hotspots may indicate the existence of previously unsuspected differences in the ability of these small RNAs to interact with ARGONAUTE proteins and form stable RISC complexes.

Several groups have noted the striking similarity between the rod-like secondary structure of viroids like PSTVd and those of primary host microRNA (pri-miRNA) transcripts, and incubation of RNA transcripts derived from either PLMVd (Landry and Perreault, 2005) or PSTVd (Itaya et al., 2007) with partially-purified dicer preparations results in the release of small 21–24 nt RNAs. Furthermore, application of a recently developed computation-based approach for identifying pre-miRNA and miRNA/miRNA* sequences in plant genomes to single-stranded RNAs derived from PSTVd genomic RNA predicts formation of a prominent group of small RNAs containing sequences from the pathogenicity domain (Teune and Steger, 2010). While our analyses revealed that both Rutgers and Moneymaker plants contain just such a peak of (+)srPSTVds, they also revealed an even more prominent group of (+)srPSTVds derived from positions 95–130 in the upper portion of the central domain. Why previous analyses of infected tomato tissues (e.g., Machida et al., 2007; Itaya et al., 2007) failed to identify the upper central domain as a hotspot for (+)srPSTVd synthesis is unclear because this group of small RNAs constitute the most abundant class of (+)srPSTVd in PSTVd-infected *N. benthamiana* (DiSerio et al., 2010).

Gomez et al. (2008, 2009) have presented evidence for the existence of a dsRNA-dependent pathway for viroid small RNA synthesis, demonstrating that symptom expression in HSVd-infected *N. benthamiana* requires the activity of RDR6. RDR6 plays a key role in the synthesis of trans-acting small interfering RNAs (ta-siRNAs), catalyzing the conversion of single-stranded RNA fragments generated by miRNA-mediated cleavage of specific Pol II transcripts into double-stranded RNAs that are themselves substrates for dicer(s). In the case of PSTVd and related viroids, these authors suggest that a linear form of the genomic RNA released from multimeric replicative intermediates by dicer-mediated cleavage between positions 95–96 may be a substrate for RDR6. As predicted by Gomez et al. (2009), one of the two most abundant species of (+)srPSTVd recovered from our samples of stem tissue was a 23–25 nt RNA whose 5′ terminus is located at position 96. Its length alone points to DCL3 as the enzyme responsible for cleavage, presumably acting on partially double-stranded PSTVd replicative intermediates (Gas et al., 2007). Inspection of the region immediately downstream revealed no evidence for phased production of additional srPSTVds, however (Allen et al., 2005).

There is one additional species of srPSTVd detected in our analyses whose existence may shed light on the relative importance of single- and double-stranded PSTVd RNA as substrates for cleavage; namely, a 23–25 nt (−)srPSTVd whose 5′-terminus at position 237 is located just outside the stem of an alternative structural interaction known a "secondary hairpin II". Formed by base-pairing between positions 227–236 and 319–328, secondary hairpin II plays an important role in PSTVd replication where it appears to function primarily at the level of the antigenomic (−)strand RNA (Loss et al., 1991). We cannot yet explain the rather dramatic differences between the profiles of (−) srPSTVds recovered from Rutgers and Moneymaker plants seen in

Fig. 2, and such differences could obviously have an major effect on symptom induction via RNA silencing. Nevertheless, the fact that the populations of srPSTVds isolated from infected and transgenic Moneymaker were virtually identical suggests that i) the unusually stable secondary structure of the viroid may prevent the hairpin transcript from assuming a completely double-stranded conformation and ii) structural features of the (+) and (−)strand PSTVd RNAs themselves are also important in guiding this process.

That PSTVd infection is accompanied by dramatic changes in the pattern of host gene expression is well-known, and to identify possible targets of PSTVd-mediated RNA silencing we employed a microarray-based approach. At the protein level, these changes include accumulation of pathogenesis-related (PR) proteins such as PR-1b (Camacho-Henriquez and Sänger, 1984) and induction of at least two different protein kinases (Hiddinga et al., 1988; Hammond and Zhao, 2000). A previous study by Itaya et al. (2002) used cDNA macroarrays to monitor changes in host gene expression at different stages of the infection process, thereby revealing a complex pattern of changes involving defense/stress responses, cell wall and protein metabolism, and chloroplast function. The availability of Affymetrix tomato arrays containing probe sets for ~10,000 genes allowed us to monitor nearly 10-fold more genes than this earlier study, and analysis of the resulting data indicated that expression levels of approximately one in four tomato genes are significantly affected by PSTVd infection — an effect several-fold greater than that previously reported. Based on a genome sequence that is approximately 50% complete, more than 100 genes on the Affymetrix array contain potential binding sites for srPSTVds.

PSTVd infection appeared to have no significant effect on the expression of almost two-thirds of these genes, and transcript levels for less than half of the remaining 42 genes were down-regulated in infected (and severely diseased) Rutgers plants. The proteins encoded by the 18 down-regulated genes represent a diverse collection of enzymes and regulatory proteins, two of which (i.e., gibberellin beta-hydroxylase and a metal ion-binding, copper chaperone (CCH)-related protein) were also down-regulated in both PSTVd-infected and transgenic Moneymaker plants. In assessing the likelihood that this down-regulation involves RNA silencing we note that both predicted srPSTVds are associated with known hotspots on the more abundant PSTVd genomic strand. For gibberellin beta-hydroxylase this hotspot is located in the upper portion of the variable region; for the metal ion-binding protein, the corresponding hotspot lies within the pathogenicity domain. A third potential target gene of interest is an omega-3 fatty acid desaturase that is involved in the synthesis of linolenic acid, a precursor to jasmonic acid. In this case, however, mRNA levels in the transgenic Moneymaker plants were not significantly down-regulated.

Stunting is often considered a diagnostic feature for viroid infection of certain hosts like tomato (Diener, 1987). PSTVd-infected plants might thus be expected to exhibit changes in the levels of mRNAs encoding enzymes involved in gibberellin biosynthesis, and gibberellin beta-hydroxylase is involved in the conversion of inactive to bioactive gibberellins (Hammond and Zhao, 2009). The ORF of omega-3 fatty acid desaturase also contains a potential target for (+) srPSTVd, in this case originating from a hotspot in the lower portion of the central domain. Many defense responses to virus infection by compatible hosts are dependent on salicylic acid signaling, with apparently less input from the jasmonic acid/ethylene pathway (Whitam et al., 2006; Wise et al., 2007). Additional studies are required to determine whether any of the down-regulated mRNAs identified by microarray analysis are cleaved at the predicted target sites, and the results of such studies will clarify the relative importance of (+) and (−) srPSTVd in disease induction. One question of particular interest involves the symptoms that we have observed in transgenic Moneymaker line IR14 growing under greenhouse conditions. Schwind et al. (2009) have reported that several other transgenic lines containing the same non-infectious PSTVd cDNA hairpin and expressing apparently similar arrays of srPSTVds fail to show the severe stunting and epinasty that we have observed for line IR14. None of these transgenic lines have been well-characterized with respect to the copy number and location(s) of their PSTVd cDNA inserts, and thus we cannot explain this discrepancy at the present time. At the very least, however, such transgenic plants can provide useful controls for future experiments.

An important question not addressed in the current study concerns the possible effect of PSTVd-induced changes in host miRNA populations on normal patterns of PTGS. Several recent reviews (e.g., Ruiz-Ferrer and Voinnet, 2009; Umbach and Cullen, 2009) discuss the role of virus-induced miRNA changes in modulating symptom production and other aspects of virus–host interaction. A recently published study involving six RNA viruses and forty-one vertebrate and invertebrate hosts (Parameswaran et al., 2010) used large-scale sequencing to monitor changes in populations of both virus-specific and host small RNAs following infection. No plant viruses were included in these studies which took advantage of several cell lines in which key components of the RNAi and interferon signaling pathways had been inactivated by mutation, but taking particular care to properly normalize their data these authors report several instances in which the ratio of small RNA derived from the genomic and antigenomic strands appeared to vary widely. Preliminary analysis of the host-specific small RNAs captured by our analyses (Owens RA, Tech KB, Shao JY, Sano T, and Baker CJ, unpublished data) indicates that, PSTVd infection (like those involving conventional RNA or DNA viruses) is also accompanied by cultivar-dependent changes in host miRNAs levels. Work is currently underway to assess the relative importance of these different aspects of PTGS in regulating the interaction between PSTVd and its many hosts.

Materials and methods

Viroid inoculation and small RNA extraction

Tomato (*Solanum lycopersicum*, cv. Rutgers) seedlings were inoculated with PSTVd (ca. 2 ng in 10 µl 20 mM Na phosphate, pH 7.0) at the cotyledon stage and incubated in a growth chamber maintained at 24 °C with 16 h day-length and supplemental high intensity sodium lighting. Three and four weeks post inoculation (w.p.i.), individual leaves and internodes (from the lowest to the uppermost) were collected from 4 to 6 plants, and pooled tissue samples were processed for extraction of low molecular weight RNA soluble in 2 M LiCl (LMW-RNA) for detection of PSTVd-specific small RNAs (srPSTVds) (Sano and Matsuura, 2004; Machida et al., 2007, 2008). Briefly, freshly collected leaf or stem tissue was ground in a mortar and pestle with five volumes (w/v) of extraction buffer containing 0.1 M Tris–HCl (pH 9.5) – 0.01 M EDTA (pH 7.0) – 1.5 M NaCl – 0.4% 2-mercaptoethanol – 2% cetytrimethylammonium bromide – 10 U/ml Ribonuclease inhibitor (Wako — Osaka, Japan), extracted with equal volume of phenol:chloroform (1:1, v/v) mixture, fractionated by 2 M LiCl treatment, and treated with RNase-free DNase I (Promega — WI, USA) according to the manufacturer's instruction.

Northern analysis of viroid genomic and small RNAs

Samples of LMW-RNA (ca. 2 µg) were dissolved in 10 µl aliquots of loading buffer containing 25% (w/v) urea, 10% (v/v) glycerol and 0.01% each of bromophenol blue and xylene cyanol FF. After heat denaturation (68 °C, 15 min), these samples were fractionated by electrophoresis in 7.5% polyacrylamide gels (acrylamide:bisacrylamide = 39:1) for genomic RNA or 12% polyacrylamide gels (acrylamide:bisacrylamide = 19:1) for small RNAs, both containing 1× TBE

buffer and 8 M urea. RNAs were then transferred to a nylon membrane (Biodyne Plus — Pall) and hybridized with DIG-labeled cRNA probes to detect either genomic RNA, or PSTVd-specific small RNAs of both polarities (srPSTVds) (Machida et al., 2007). Northern hybridization signals were visualized using a Chemidoc-XRS (Bio-Rad) imaging system (1–2 h exposure) and quantified using the Quantity One (version 4.6.2) software package. These experiments were repeated three times, and, where indicated, analyses included a set of ssRNA size markers having lengths of 14, 18, 22, 26, and 30 nt (Takara Bio — Ohtsu, Japan).

Large-scale sequencing

In initial experiments small RNAs were purified from preparations of LMW RNA isolated from individual leaves and stem segments of PSTVd-infected Rutgers tomatoes harvested 3 wpi by electrophoresis in 12% polyacrylamide gels containing 8 M urea. Following fractionation a nylon membrane (Biodyne Plus) was placed on the gel overnight, cross-linked by UV irradiation after removal, and then hybridized with DIG-labeled PSTVd-cRNA probes to detect srPSTVds. After visualization of hybridization signals on Hyper film (Amersham), small RNAs containing ca. 15–30 nt were excised, eluted overnight in 0.5 M ammonium acetate – 0.1% SDS, precipitated with ethanol, and finally dissolved in 20 µl RNase-free water. Samples were sent to Hokkaido System Science (Sapporo, Japan) for the large scale sequence analysis using a Genetic Analyzer II (Illumina — San Diego, CA) and reagents/protocols supplied by the manufacturer. In later experiments involving microarray analysis (see below), small RNAs were purified from total leaf RNA preparations extracted from leaf tissue using TRI reagent.

Adapter sequences were removed from the ends of the resulting raw short-read data based on the presence of an exact 10-nt match with the termini of the respective adapters, and identical short reads were grouped according to read size (15–29 nt). In this way, adapter-trimmed short read data was converted to a non-redundant "short-read-sequence occurrence" format. These non-redundant data were then mapped to either the genomic or anti-genomic strand of PSTVd using *hssmap*, a specially-written C language program that processes data from circular molecules by adding an appropriate extension to the 3′ terminus of a linear reference sequence. Executable files for Linux, Mac OS X, and Windows versions of this program can be downloaded from our website [http://rna.eit.hirosaki-u.ac.jp/hssmap/].

mRNA profiling

The terminal leaflet on the third leaf of greenhouse-grown Rutgers or Moneymaker seedlings containing 3–4 true leaves was dusted with carborundum and inoculated with a 10 µl aliquot of either 20 mM Na phosphate, pH 7.0 (buffer control) or the same solution containing ~100 ng ribozyme-derived, precisely-full-length PSTVd_Intermediate strain RNA transcripts (Feldstein et al., 1998). Comparable seedlings of transgenic Moneymaker line IR11-14 (Wang et al., 2004) were left uninoculated. Plants were returned to the greenhouse, and 27 days later systemically-infected tissue from leaf 11 was collected from four individual plants for extraction of total RNA and microarray analysis. Fresh leaf tissue from each biological replicate was frozen in liquid nitrogen, powdered in a mortar and pestle, and extracted with TRI reagent as recommended by the manufacturer (Molecular Research Center — Cincinnati, OH). Aliquots (100 µg) of the resulting total RNA preparations were applied to RNeasy columns, incubated with RNase-free DNase, and eluted in sterile deionized water as recommended by the manufacturer (Qiagen — Valencia, CA). In addition to Rutgers these assays also included both transformed and non-transformed Moneymaker plants. Transformed Moneymaker line 1R14 (Wang et al., 2004) is resistant to PSTVd infection and constitutively expresses srPSTVd from a non-infectious hairpin cDNA (Schwind et al., 2009).

mRNA profiling analysis using Affymetrix oligonucleotide probe arrays (Affymetrix — Santa Clara, CA) was carried out at the Biopolymer-Genomics Core Facility operated by the University of Maryland School of Medicine (Baltimore, MD). Double-stranded cDNA was synthesized from DNA-free tomato total RNA (1–2 µg) using One-Cycle Target Labeling and Control Reagents (Affymetrix). Biotin-labeled cRNA (15 µg) synthesized in the subsequent *in vitro* transcription reaction was fragmented before hybridization to the genome arrays. In addition to fragmented target cRNA, the hybridization solution also contained BSA, herring sperm DNA, and probe array control RNAs from the kit. Following 16 h incubation at 45 °C, the probe array was immediately processed using an Affymetrix FS-450 fluidics station and an automated washing and staining protocol (EukGE-WS2v5). Stained arrays were scanned using an Affymetrix GeneChip Scanner 7000.

Microarray data analysis

Tomato GeneChip scanning data were analyzed at probe-level to directly extract signal intensities from .CEL files using the Jmp Genomics v.3.2 software package (SAS Institute — Cary, NC). A Robust Multichip Average (RMA) background correction was applied to each array, and the data was then log 2 transformed. Next, the data sets were quantile normalized and summarized using the MEDIANPOLISH function. To identify genes significantly affected by PSTVd infection, the data was processed using a One-Way ANOVA model that compared infected to healthy plants using a False Discovery Rate testing method [alpha = .01]. MIAME-compliant data files are available from the Tomato Functional Genomics Database (http://ted.bti.cornell.edu).

Identification of potential PSTVd small RNA target sites

Sequences of the PSTVd genomic and anti-genomic RNA were each divided into a series of 359 non-overlapping oligonucleotides, each 21 nucleotides in length. Groups of 10 such short RNAs were submitted to the Tomato Functional Genomics Database (http://ted.bti.cornell.edu) to locate potential target sites in Tomato Unigene Build 2 using an algorithm developed by Jones-Rhoades and Bartel (2004). The resulting lists of target genes were then compared to the list of genes represented on the Affymetrix tomato array, and the location of each "hit" (i.e., 5′-UTR, coding region, or 3′-UTR) was determined.

Supplementary materials related to this article can be found online at doi:10.1016/j.virol.2011.01.021.

Acknowledgments

Seeds of several transgenic Moneymaker tomato lines including IR11-11 and IR11-14 were provided by Dr. Ming-Bo Wang (CSIRO — Canberra). We thank Kim Tech and Jonathan Shao (MPPL) for expert assistance in analysis of microarray data and examination of the tomato genome for potential srPSTVd target sites. Microarray analyses were performed by Jing Yin (University of Maryland School of Medicine), and Doug Robinson (SAS — Cary, NC) provided invaluable advice and assistance in the use of the Jmp Genomics software package. We also thank Naoyuki Sugimoto and Shiho Ishii (Hokkaido System Science Co. Ltd., Sapporo, Japan) for technical assistance of Illumina Genome Analyzer. This work was supported in part by Grants-in Aid for Scientific Research B18380028, 21380029 and 18658016 from Japan Society for the Promotion of Science, and Grant-in Aid-for Scientific Research of Priority Area, Hirosaki University 2008. This work was done in part at Gene Research Center, Hirosaki University.

References

Allen, E., Xie, Z., Gustafson, A.M., Carrington, J.C., 2005. microRNA-directed phasing during *trans*-acting siRNA biogenesis in plants. Cell 121, 207–221.

Baulcombe, D., 2004. RNA silencing in plants. Nature 431, 356–363.

Baumstark, T., Schröder, A.R.W., Riesner, D., 1997. Viroid processing: switch from cleavage to ligation is driven by a change from a tetraloop to a loop E conformation. EMBO J. 16, 599–610.

Bolduc, F., Hoareau, C., St-Pierre, P., Perreault, J-P., 2010. In-depth sequencing of the siRNAs associated with peach latent mosaic viroid infection. BMC Mol. Biol. 11, 16.

Branch, A.D., Robertson, H.D., 1984. A replication cycle for viroids and other small infectious RNA's. Science 223, 450–455.

Camacho-Henriquez, A., Sänger, H.L., 1984. Purification and partial characterization of the major "pathogenesis-related" tomato leaf protein P14 from potato spindle tuber viroid (PSTV)-infected tomato leaves. Arch. Virol. 81, 263–284.

Carbonell, A., Martínez de Alba, A.E., Flores, R., Gago, S., 2008. Double-stranded RNA interferes in a sequence-specific manner with the infection of representative members of the two viroid families. Virology 371, 44–53.

Daros, J.A., Flores, R., 2004. *Arabidopsis thaliana* has the enzymatic machinery for replicating representative viroid species of the family *Pospiviroidae*. Proc. Natl Acad. Sci. USA 101, 6792–6797.

Daros, J.A., Elena, S.F., Flores, R., 2006. Viroids: an Ariadne's thread into the RNA labyrinth. EMBO Rep. 7, 593–598.

Diener, T.O., 1986. Viroid processing: a model involving the central conserved region and hairpin I. Proc. Natl Acad. Sci. USA 83, 58–62.

Diener, T.O., 1987. Biological properties. In: Diener, T.O. (Ed.), The Viroids. Plenum Press, New York, USA, pp. 9–35.

Ding, B., Itaya, A., 2007. Viroid: a useful model for studying the basic principles of infection and RNA biology. Mol. Plant-Microbe Interact. 20, 7–20.

Ding, S.W., 2010. RNA-based antiviral immunity. Nat. Rev. Immunol. 10, 632–644.

Di Serio, F., Gisel, A., Navarro, B., Delgado, S., Martínez de Alba, Á.-E., Donvito, G., Flores, R., 2009. Deep sequencing of the small RNAs derived from two symptomatic variants of a chloroplastic viroid: implications for their genesis and for pathogenesis. PLoS ONE 4 (10), e7539. doi:10.1371/journal.pone.0007539.

Di Serio, F., Martínez de Alba, A.E., Navarro, B., Gisel, A., Flores, R., 2010. RNA-dependent RNA polymerase 6 delays accumulation and precludes meristem invasion of a viroid that replicates in the nucleus. J. Virol. 84, 2477–2489.

Elbashir, S.M., Lendeckel, W., Tsuchl, T., 2001. RNA interference is mediated by 21- and 22-nucleotide RNAs. Genes Dev. 15, 188–200.

Feldstein, P.A., Hu, Y., Owens, R.A., 1998. Precisely full length, circularizable, complementary RNA: an infectious form of potato spindle tuber viroid. Proc. Nat. Acad. Sci. U.S.A. 95, 6560–6565.

Flores, R., Hernandez, C., Martinez de Alba, A.E., Daros, J.A., Di Serio, F., 2005a. Viroids and viroid–host interactions. Annu. Rev. Phytopathol. 43, 117–139.

Flores, R., Randles, J.W., Owens, R.A., Bar-Joseph, M., Diener, T.O., 2005b. Viroids. In: Fauquet, C.M., Mayo, M.A., Maniloff, J., Desselberger, U., Ball, L.A. (Eds.), Virus Taxonomy — Classification and Nomenclature of Viruses (Eighth Report of the International Committee on the Taxonomy of Viruses). Elsevier, London, pp. 1147–1161.

Fusaro, A.F., Matthew, L., Smith, N.A., Curtin, S.J., Dedic-Hagan, J., Ellacott, G.A., Watson, J.M., Wang, M.B., Brosnan, C., Carroll, B.J., Waterhouse, P.M., 2006. RNA interference-inducing hairpin RNAs in plants act through the viral defence pathway. EMBO Rep. 7, 1168–1175.

Garcia-Ruiz, H., Takeda, A., Chapman, E.J., Sullivan, C.M., Fahlgren, N., Brempelis, K.J., Carrington, J.C., 2010. *Arabidopsis* RNA-dependent RNA polymerase and Dicer-like proteins in antiviral defense and small interfering RNA biogenesis during *Turnip mosaic virus* infection. Plant Cell 22, 481–496.

Gas, M.E., Hernañdez, C., Flores, R., Daròs, J.A., 2007. Processing of nuclear viroids in vivo: an interplay between RNA conformations. PLoS Pathog. 3, 1813–1826.

Gas, M.E., Molina-Serrano, D., Hernández, C., Flores, R., Daròs, J.A., 2008. Monomeric linear RNA of citrus exocortis viroid resulting from processing in vivo has 5′-phosphomonoester and 3′-hydroxyl termini: implications for the RNase and RNA ligase involved in replication. J. Virol. 82, 10321–10325.

Gómez, G., Martinez, G., Pallás, V., 2008. Viroid-induced symptoms in *Nicotiana benthamiana* plants are dependent on RDR6 activity. Plant Physiol. 148, 414–423.

Gómez, G., Martinez, G., Pallás, V., 2009. Interplay between viroid-induced pathogenesis and RNA silencing pathways. Trends Plant Sci. 14, 264–269.

Hamilton, A., Voinnet, O., Chapppell, L., Baulcombe, D., 2002. Two classes of short interfering RNA in RNA silencing. EMBO J. 21, 4671–4679.

Hammond, R.W., Zhao, Y., 2000. Characterization of a tomato protein kinase gene induced by infection by *Potato spindle tuber viroid*. Mol. Plant-Microbe Interact. 13, 903–910.

Hammond, R.W., Zhao, Y., 2009. Modification of tobacco plant development by sense and antisense expression of the tomato viroid-induced AGC VIIIa protein kinase PKV suggests involvement in gibberellin signaling. BMC Plant Biol. 9, 108. doi:10.1186/1471-2229-9-108.

Herr, A.J., 2005. Pathways through the small RNA world of plants. FEBS Lett. 579, 5879–5888.

Hiddinga, H.J., Crum, C.J., Hu, J., Roth, D.A., 1988. Viroid-induced phosphorylation of a host protein related to a dsRNA-dependent protein kinase. Science 241, 451–453.

Itaya, A., Folimonov, A., Matsuda, Y., Nelson, R.S., Ding, B., 2001. Potato spindle tuber viroid as inducer of RNA silencing in infected tomato. Mol. Plant-Microbe Interact. 14, 1332–1334.

Itaya, A., Matsuda, Y., Gonzales, R.A., Nelson, R.S., Ding, B., 2002. Potato spindle tuber viroid strains of different pathogenicity induces and suppresses expression of common and unique genes in infected tomato. Mol. Plant-Microbe Interact. 15, 990–999.

Itaya, A., Zhong, X., Bundschuh, R., Qi, Y., Wang, Y., Takeda, R., Harris, A.R., Molina, C., Nelson, R.S., Ding, B., 2007. A structured viroid RNA is substrate for dicer-like cleavage to produce biologically active small RNAs but is resistant to RISC-mediated degradation. J. Virol. 81, 2980–2994.

Jones-Rhoades, M.W., Bartel, D.P., 2004. Computational identification of plant microRNAs and their targets, including a stress-induced miRNA. Mol. Cell 14, 787–799.

Keese, P., Symons, R.H., 1985. Domains in viroids: evidence of intermolecular RNA rearrangements and their contribution to viroid evolution. Proc. Natl Acad. Sci. USA 82, 4582–4586.

Landry, P., Perreault, J.P., 2005. Identification of a peach latent mosaic viroid hairpin able to act as a Dicer-like substrate. J. Virol. 79, 6540–6543.

Loss, P., Schmitz, M., Steger, G., Riesner, D., 1991. Formation of a thermodynamically metastable structure containing hairpin II is critical for infectivity of potato spindle tuber viroid RNA. EMBO J. 10, 719–727.

Machida, S., Yamahata, N., Watanuki, H., Owens, R.A., Sano, T., 2007. Successive accumulation of two size classes of viroid-specific small RNA in potato spindle tuber viroid-infected tomato plants. J. Gen. Virol. 88, 3452–3457.

Machida, S., Shibuya, M., Sano, T., 2008. Enrichment of viroid small RNAs by hybridization selection using biotinylated RNA transcripts to analyze viroid induced RNA silencing. J. Gen. Plant Pathol. 74, 204–207.

Martín, R., Arenas, C., Daròs, J.A., Covarrubias, A., Reyes, J.L., Chua, N.H., 2007. Characterization of small RNAs derived from citrus exocortis viroid (CEVd) in infected tomato plants. Virology 367, 135–146.

Markarian, N., Li, H.E., Ding, S.W., Semancik, J.S., 2004. RNA silencing as related to viroid-induced symptom expression. Arch. Virol. 149, 397–406.

Martinez, G., Donaire, L., Llave, C., Pallas, V., Gomez, G., 2010. High-throughput sequencing of *Hop stunt viroid*-derived small RNAs from cucumber leaves and phloem. Mol. Plant Pathol. 11, 347–359.

Martinez de Alba, A.E., Flores, R., Hernandez, C., 2002. Two chloroplastic viroids induce the accumulation of the small RNAs associated with post-transcriptional gene silencing. J. Virol. 76, 13094–13096.

Matoušek, J., Kozlová, P., Orctová, L., Schmitz, A., Pesina, K., Bannach, O., Diermann, N., Steger, G., Riesner, D., 2007. Accumulation of viroid-specific small RNAs and increase in nucleolytic activities linked to viroid-caused pathogenesis. Biol. Chem. 388, 1–13.

Moissiard, G., Voinnet, O., 2006. RNA silencing of host transcripts by cauliflower mosaic virus requires coordinated action of four *Arabidopsis* Dicer-like proteins. Proc. Natl Acad. Sci. USA 103, 19593–19598.

Molnar, A., Csorba, T., Lakatos, L., Varallysy, E., Lacomme, C., Burgyan, J., 2005. Plant virus-derived small interfering RNAs originate predominantly from highly structured single-stranded viral RNAs. J. Virol. 79, 7812–7818.

Molnar, A., Melnyk, C.W., Bassett, A., Hardcastle, T.J., Dunn, R., Baulcombe, D.C., 2010. Small silencing RNAs in plants are mobile and direct epigenetic modification in recipient cells. Science 328, 872–875.

Navarro, B., Pantaleo, V., Gisel, A., Moxon, S., Dalmay, T., et al., 2009. Deep sequencing of viroid-derived small RNAs from grapevine provides new insights on the role of RNA silencing in plant-viroid interaction. PLoS ONE 4 (11), e7686. doi:10.1371/journal.pone.0007686.

Papaefthimiou, I., Hamilton, A.J., Denti, M.A., Baulcombe, D.C., Tsagris, M., Tabler, M., 2001. Replicating potato spindle tuber viroid RNA is accompanied by short RNA fragments that are characteristic of posttranscriptional gene silencing. Nucleic Acids Res. 29, 2395–2400.

Parameswaran, P., Sklan, E., Wilkins, C., Burgon, T., Samuel, M.A., et al., 2010. Six RNA viruses and forty-one hosts: viral small RNAs and modulation of small RNA repertoires in vertebrate and invertebrate systems. PLoS Pathog. 6 (2), e1000764. doi:10.1371/journal.ppat.1000764.

Qi, Y., Ding, B., 2003. Inhibition of cell growth and shoot development by a specific nucleotide sequence in a noncoding viroid RNA. Plant Cell 15, 1360–1374.

Reanwarakorn, K., Semancik, J.S., 1998. Regulation of pathogenicity in hop stunt viroid-related group II citrus viroids. J. Gen. Virol. 79, 3163–3171.

Rodriguez, M.J.B., Randles, J.W., 1993. Coconut cadang-cadang viroid (CCCVd) mutants associated with severe diseases vary in both the pathogenicity domain and central conserved region. Nucleic Acids Res. 21, 2771.

Ruiz-Ferrer, V., Voinnet, O., 2009. Roles of plant small RNAs in biotic stress responses. Annu. Rev. Plant Biol. 60, 485–510.

Sano, T., Candresse, T., Hammond, R.W., Diener, T.O., Owens, R.A., 1992. Identification of multiple structural domains regulating viroid pathogenicity. Proc. Natl Acad. Sci. USA 89, 10104–10108.

Sano, T., Ishiguro, A., 1998. Viability and pathogenicity of intersubgroup viroid chimeras suggest possible involvement of the terminal right region in replication. Virology 240, 238–244.

Sano, T., Matsuura, Y., 2004. Accumulation of short interfering RNAs characteristic of RNA silencing precedes recovery of tomato plants from severe symptoms of *Potato spindle tuber viroid* infection. J. Gen. Plant Pathol. 70, 50–53.

Schnölzer, M., Haas, B., Ramm, K., Hofmann, H., Sänger, H.L., 1985. Correlation between structure and pathogenicity of potato spindle tuber viroid (PSTVd). EMBO J. 4, 2181–2190.

Schwind, N., Zwiebel, M., Itaya, A., Ding, B., Wang, M.B., Krczal, G., Wassenegger, M., 2009. RNAi-mediated resistance to Potato spindle tuber viroid in transgenic tomato expressing a viroid hairpin RNA construct. Mol. Plant Pathol. 10, 459–469.

St-Pierre, P.I., Hassen, F., Thompson, D., Perreault, J.P., 2009. Characterization of the siRNAs associated with peach latent mosaic viroid infection. Virology 383, 178–182.

Tabler, M., Tsagris, M., 2004. Viroids: petite RNA pathogens with distinguished talents. Trends Plant Sci. 9, 339–348.

Teune, J.-H., Steger, G., 2010. NOVOMIR: de novo prediction of microRNA-coding regions in a single plant genome. J. Nuc. Acids. doi:10.4061/2010/495904 Article ID 495904.
Umbach, J.L., Cullen, B.R., 2009. The role of RNAi and microRNAs in animal virus replication and antiviral immunity. Genes Dev. 23, 1151–1164.
Vance, V., Vaucheret, H., 2001. RNA silencing in plants — defense and counterdefense. Science 292, 2277–2280.
Visvader, J.E., Symons, R.H., 1985. Eleven new sequence variants of citrus exocortis viroid and the correlation of sequence with pathogenicity. Nucleic Acids Res. 13, 2907–2920.
Wang, M.B., Bian, X.Y., Wu, L.M., Liu, L.X., Smith, N.A., Isenegger, D., Wu, R.M., Masuta, C., Vance, V.B., Watson, J.M., Rezaian, A., Dennis, E.S., Waterhouse, P.M., 2004. On the role of RNA silencing in the pathogenicity and evolution of viroids and viral satellites. Proc. Natl Acad. Sci. USA 101, 3275–3280.
Whitham, S.A., Yang, C., Goodin, M.M., 2006. Global impact: elucidating plant responses to viral infection. Mol. Plant-Microbe Interact. 19, 207–215.
Wise, R.P., Moscou, M.J., Bogdanove, A.J., Whitham, S.A., 2007. Transcript profiling in host–pathogen interactions. Annu. Rev. Phytopathol. 45, 329–369.